

# Minimization of Loss in Small Scale Axial Air Turbine Using CFD Modelling and Evolutionary Algorithm Optimization

Bahr Ennil, Ali; Al-Dadah, Raya; Mahmoud, Saad; Rahbar, Kiyarash; Al Jubori, Ayad

DOI:

[10.1016/j.applthermaleng.2016.03.077](https://doi.org/10.1016/j.applthermaleng.2016.03.077)

License:

Creative Commons: Attribution-NonCommercial-NoDerivs (CC BY-NC-ND)

*Document Version*

Peer reviewed version

*Citation for published version (Harvard):*

Bahr Ennil, A, Al-Dadah, R, Mahmoud, S, Rahbar, K & Al Jubori, A 2016, 'Minimization of Loss in Small Scale Axial Air Turbine Using CFD Modelling and Evolutionary Algorithm Optimization', *Applied Thermal Engineering*, vol. 102, pp. 841-8. <https://doi.org/10.1016/j.applthermaleng.2016.03.077>

[Link to publication on Research at Birmingham portal](#)

**Publisher Rights Statement:**

Checked April 2016

**General rights**

Unless a licence is specified above, all rights (including copyright and moral rights) in this document are retained by the authors and/or the copyright holders. The express permission of the copyright holder must be obtained for any use of this material other than for purposes permitted by law.

- Users may freely distribute the URL that is used to identify this publication.
- Users may download and/or print one copy of the publication from the University of Birmingham research portal for the purpose of private study or non-commercial research.
- User may use extracts from the document in line with the concept of 'fair dealing' under the Copyright, Designs and Patents Act 1988 (?)
- Users may not further distribute the material nor use it for the purposes of commercial gain.

Where a licence is displayed above, please note the terms and conditions of the licence govern your use of this document.

When citing, please reference the published version.

**Take down policy**

While the University of Birmingham exercises care and attention in making items available there are rare occasions when an item has been uploaded in error or has been deemed to be commercially or otherwise sensitive.

If you believe that this is the case for this document, please contact [UBIRA@lists.bham.ac.uk](mailto:UBIRA@lists.bham.ac.uk) providing details and we will remove access to the work immediately and investigate.

1  
2 **Minimization of Loss in Small Scale Axial Air Turbine Using CFD**  
3 **Modelling and Evolutionary Algorithm Optimization**

4  
5 Ali Bahr Ennil<sup>a,\*</sup>, Raya Al-Dadah<sup>a</sup>, Saad Mahmoud<sup>a</sup>, Kiyarash Rahbar<sup>a</sup>, Ayad AlJubori<sup>a</sup>

6 <sup>a</sup>School of Mechanical Engineering

7 University of Birmingham, Edgbaston, Birmingham, United Kingdom, B15-2TT

8 \* Corresponding author. E-mail: [asb208@bham.ac.uk](mailto:asb208@bham.ac.uk).

---

9  
10 **Abstract:**

11 Small scale axial air driven turbine (less than 10kW) is the crucial component in  
12 distributed power generation cycles and in compressed air energy storage systems driven by  
13 renewable energies. Efficient small axial turbine design requires precise loss estimation and  
14 geometry optimization of turbine blade profile for maximum performance. Loss predictions  
15 are vital for improving turbine efficiency. Published loss prediction correlations were  
16 developed based on large scale turbines; therefore, this work aims to develop a new approach  
17 for losses prediction in a small scale axial air turbine using computational fluid dynamics  
18 (CFD) simulations. For loss minimization, aerodynamics of turbine blade shape was  
19 optimized based on fully automated CFD simulation coupled with Multi-objective Genetic  
20 Algorithm (MOGA) technique. Compare to other conventional loss models, results showed  
21 that the Kacker & Okapuu model predicted the closest values to the CFD simulation results  
22 thus it can be used in the preliminary design phase of small axial turbine which can be further  
23 optimised through CFD modelling. The combined CFD with MOGA optimization for  
24 minimum loss showed that the turbine efficiency can be increased by 12.48% compare to the  
25 baseline design.

26 **Keywords:** Small Scale Axial turbine, CFD, Total Loss, Optimization, Genetic algorithm.

30 **Nomenclature:**

31

$Y_{total}$	Total Loss Coefficient	[-]	$s$	Blade Spacing	[mm]
$Y_{Tl}$	Trailing Loss coefficient	[-]	$\Delta\eta$	Efficiency change	[-]
$Y_p$	Profile Loss Coefficient	[-]	$\eta_o$	Efficiency at zero clearance	[-]
$Y_s$	Secondary Loss Coefficient	[-]	$\eta_{tt}$	Total to total efficiency	[-]
$Y_k$	Tip Clearance Loss	[-]	$\alpha_{in}$	Inlet flow angle	[Degree]
$Y_{shock}$	Loss due to shocks	[-]	$\alpha_{out}$	Exit flow angle	[Degree]
$Y_N$	Nozzle Pressure Loss Coefficient	[-]	$\alpha_m$	mean angle	[Degree]
$Y_R$	Rotor Pressure Loss Coefficient	[-]	$\varepsilon$	Blade Deflection Angle	[Degree]
$X_{Te}$	Trailing Edge Correction factor	[-]	$R_e$	Reynolds number	[-]
$x_i$	Incidence factor	[-]	$M_{in}$	Inlet Mach number	[-]
$X_{Re}$	Loss correction factor	[-]	$X_{AR}$	Aspect ratio coefficient	[-]
$\Delta E_{Te}$	Energy loss coefficient at TE	[-]	$k'$	Effective tip clearance	[mm]
$K_P$	Mach number Factor	[-]	$M_{out}$	Exit Mach number	[-]
$\zeta^*$	Nominal loss factor	[-]	$h_{o1}$	Total Inlet Enthalpy	[J/kg.K]
$\zeta_N$	Nozzle Loss Coefficient	[-]	$h_{o3}$	Total Exit Enthalpy	[J/kg.K]
$\zeta_R$	Rotor Loss Coefficient	[-]	$h_3$	Static Exit Enthalpy	[J/kg.K]
$L$	Lift Force	[N]	$C_2$	Nozzle Exit Absolute Velocity	[m/sec]
$D$	Drag Force	[N]	$W_3$	Rotor Exit Relative Velocity	[m/sec]
$C_L$	Lift Coefficient	[-]	$S$	Entropy	[J/kg.K]
$C_D$	Drag Coefficient	[-]	$T_3$	Exit Static Temperature	[K]
$\tau$	Tip clearance	[mm]	$P_o$	Total Pressure	[Pa]
$H$	Blade height	[mm]	$P$	Static Pressure	[Pa]
$c$	Blade chord	[mm]	$OF$	Objective Function	[-]
$V_\infty$	Main stream velocity	[m/sec]	$r_H$	Hub radius	[mm]
$P_{in}$	Inlet pressure	[Pa]	$r_T$	Tip radius	[mm]
$P_{out}$	Outlet pressure	[Pa]			

32

33

34 **1. Introduction:**

35 The availability of efficient small scale axial air turbines (less than 10kW) is vital for  
 36 the development of renewable energy systems like the solar thermal air driven Brayton cycle  
 37 [1, 2] and small scale compressed air energy storage systems [3, 4], where compressed air can  
 38 be used to drive air turbines and generate power output.

39 The preliminary design phase of axial turbines starts with one dimensional mean line  
 40 calculations which assume that the flow can be represented at turbine blade mid-span.  
 41 Detailed description about mean line design approach is provided by many text-books e.g. [5-  
 42 7] and some parameters selections are left to the designer for optimum blade configuration. In  
 43 conventional turbine design, the one dimensional mean line approach is followed by through  
 44 flow analysis or 2D inviscid design calculations to consider the variations in flow along

45 turbine blade span. The through flow analysis can be conducted in the case of large scale  
46 turbines with long blades with hub to tip ratio around 0.4 where the variations in flow are  
47 significant [8, 9].

48 Axial turbine performance prediction based on loss estimation using Ainely- Mthieson [10]  
49 correlations is the most widely used method in turbine design [11, 12]. This approach was  
50 improved by Dunham and Came [11], also Craig and Cox [12] proposed an improved  
51 correlations for losses prediction. Ainely- Mthieson correlations are based on many  
52 simplified assumptions and some tests of blade loss prediction for typical conventional gas  
53 turbine blades of 50's with large blade sections [13] According to Craig & Cox [13] the use  
54 of traditional performance estimation methods (e.g. Ainely, Traaupel, Smith Chart, and  
55 Soderberg) in steam turbine design leads to unsuccessful results and improvements for loss  
56 predictions is required. Moustapha et al. [14] carried out a review of existing correlations for  
57 losses prediction and concluded Ainely- Mthieson correlations are less tolerant for recent  
58 turbine designs.

59 In general, the published losses predictions correlations have been developed for large  
60 scale turbines, but as turbine sizes get smaller the effect of aerodynamic losses becomes more  
61 significant, therefore, the development of more accurate loss prediction models is required for  
62 small scale turbines [15, 16].

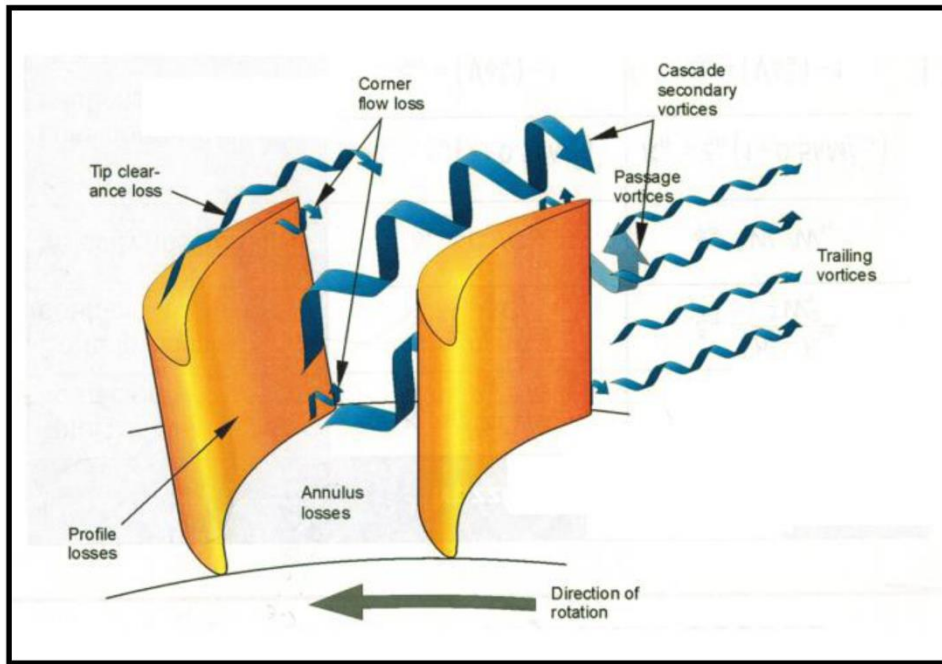
63 Limited studies have been conducted to develop means for loss prediction in small  
64 scale axial turbines [17-19]. Therefore this work aims to develop a new approach to predict  
65 the losses in a small scale axial air turbine using computational fluid dynamics (CFD)  
66 simulations.

67  
68  
69

70 **2. Axial Turbine Losses:**

71 Efficient axial turbine design requires understanding of the aerodynamic losses  
72 generated due to the complex 3-D viscous flow through the turbine. These losses are  
73 classified as shown in Figure 1 into:

74  
75  
76  
77  
78  
79  
80  
81  
82  
83  
84  
85  
86  
87  
88  
89  
90  
91  
92  
93  
94  
95  
96  
97



98  
99  
100 **Figure 1: Loss Sources in Axial Turbine [6]**

- 101 • **Profile Loss:** This loss is generated by the boundary layer formation due to the viscosity  
102 effect. The growth of this boundary layer is related to blade shape which causes boundary  
103 layer separation in some cases.
- 104 • **Annulus Loss:** This loss represents the skin friction loss at the end walls of turbine blade  
105 rows.
- 106 • **Secondary Loss:** This loss occurs near to the end walls boundary layer where the flow is  
107 turned due to pressure gradient and flow vortices are generated as a result of mixing  
secondary flow and main flow.

108 • **Tip Clearance Loss:** This loss occurs in the region between moving blades and casing  
109 leading to flow leakage. In tip clearance regions the leakage flow and main flow are mixed  
110 leading to vortex generation.

### 111 3. Axial Turbine Loss Coefficients:

112  
113 To assess the losses occurring during expansion through the turbine, there are three loss  
114 coefficients which are related to the reduction in flow enthalpy compared with isentropic  
115 enthalpy [20]. These loss coefficients include:

116 • **Energy Loss Coefficient:** based on energy conservation law this coefficient defines  
117 the amount of energy that does not contribute to the generation of work [21].

$$\zeta_N = \frac{(h_3 - h_{3S})}{\frac{1}{2} C_{2s}^2} \quad (1)$$

$$\zeta_R = \frac{(h_3 - h_{3S})}{\frac{1}{2} W_{3s}^2} \quad (2)$$

118

119 This loss coefficient is another way of defining turbine efficiency which can be defined  
120 as:

$$\eta_{tt} = \frac{h_{o1} - h_{o3}}{h_{o1} - h_{o3ss}} \quad (3)$$

121

122 • **Entropy Loss Coefficient:** It is another way to define isentropic efficiency and it is  
123 expressed in terms of entropy change instead of enthalpy change based on second law  
124 of thermodynamics [21].

$$\zeta_N = \frac{(S_2 - S_1) \cdot T_3}{\frac{1}{2} C_2^2} \quad (4)$$

$$\zeta_R = \frac{(S_3 - S_2) \cdot T_3}{\frac{1}{2} W_3^2} \quad (5)$$

125

- 126 • **Pressure Loss Coefficient:** it is a measure of loss in total pressure through turbine  
127 blades [21].

$$Y_N = \frac{(P_{01} - P_{02})}{(P_{02} - P_2)} \quad (6)$$

$$Y_R = \frac{(P_{02 \text{ rel}} - P_{03 \text{ rel}})}{(P_{01 \text{ rel}} - P_3)} \quad (7)$$

128

129 According to Moustapha [14] the total loss coefficient ( $Y_{total}$ ) can be converted into  
130 kinetic energy loss as:

131

$$Y_{total} = \frac{\left[1 - \frac{\gamma - 1}{2} M_{out}^2 \left(\frac{1}{\phi^2} - 1\right)\right]^{-\left(\frac{\gamma}{\gamma - 1}\right)} - 1}{1 - \left(1 + \frac{\gamma - 1}{2} M_{out}^2\right)^{-\left(\frac{\gamma}{\gamma - 1}\right)}} \quad (8)$$

132

133 Also, the total loss can be expressed in terms of blade aerodynamic characteristics as  
134 following [22]:

$$Y_{total} = \frac{c_D \cdot \left(\frac{C}{S}\right) \cdot \cos^2(\alpha_2)}{\cos^3(\alpha_m)} \quad (9)$$

$$C_L = \frac{L}{\frac{1}{2} \rho V_\infty^2 C} \quad (10)$$

$$C_D = \frac{D}{\frac{1}{2} \rho V_\infty^2 C} \quad (11)$$

135

136

137

138

## 139 **4. Review of Existing Loss Prediction Correlations:**

140

### 141 **4.1. Soderberg Model:**

142 Soderberg [8] developed a correlation to predict total profile and secondary losses but  
143 neglecting tip clearance:

$$\zeta_N = \left(\frac{10^5}{\text{Re}}\right)^{1/4} \left[ (1 + \zeta^*) \left( 0.993 + 0.075 \frac{1}{H} \right) - 1 \right] \quad (12)$$

$$\zeta_R = \left(\frac{10^5}{\text{Re}}\right)^{1/4} \left[ (1 + \zeta^*) \left( 0.975 + 0.075 \frac{1}{H} \right) - 1 \right] \quad (13)$$

144

145

146

147 Where  $\zeta^*$  = the nominal loss factor given as:

148

$$\zeta^* = 0.04 + 0.06 \left( \frac{\varepsilon}{100} \right)^2 \quad (14)$$

149

150

151

### 152 **4.2. Ainely & Mathieson Model:**

153 Using experimental data for conventional axial turbines Ainely and Mathieson [11]  
154 developed a method for losses prediction assuming that the effect of Mach number and flow  
155 outlet angles on pressure distribution can be neglected. The total losses are calculated by:

$$Y_{total} = (Y_P + Y_S + Y_{Tl}) \chi_{Te} \quad (15)$$

156

157 Where  $\chi_{Te}$  is the trailing edge correction factor,  $Y_P$  is profile loss,  $Y_S$  is secondary

158 loss, and  $Y_{Tl}$  is trailing edge loss coefficient.

$$Y_{P(i=0)} = \left\{ Y_{P(\alpha_{in}=0)} + \left( \frac{\alpha'_{in}}{\alpha_{out}} \right)^2 \left[ Y_{P(\alpha_{in}=\alpha_{out})} - Y_{P(\alpha'_{in}=0)} \right] \right\} \left( \frac{t_{max}/l}{0.2} \right)^{\frac{\alpha_{in}}{\alpha_{out}}} \quad (16)$$



$$Y_s = \lambda \left( \frac{C_L}{t/l} \right)^2 \left( \frac{\cos^2 \alpha_{out}}{\cos^3 \alpha_m} \right) \quad (17)$$

159

160 Where  $C_L$  is the lift coefficient and according to Xiao et al. [23] it can be calculated by:

$$C_L = 2 \frac{t}{l} (\tan \alpha_{in} - \tan \alpha_{out}) \cos \alpha_m \quad (18)$$

161

162

### 163 **4.3. Dunham & Came:**

164 This model modifies the Ainley & Mathieson approach by considering the influence of

165 Reynolds number on turbine losses [11].

$$Y_{total} = \left( (Y_P + Y_S) \left( \frac{Re}{2 \times 10^5} \right)^{-0.2} + Y_{Tl} \right) \chi_{Te} \quad (19)$$

$$Y_P = [1 + 60(M_{out} - 1)^2] \chi_i Y_{P(i=0)} \quad (20)$$

$$Y_S = 0.0334 \left( \frac{l}{H} \right) [4(\tan \alpha_{in} - \tan \alpha_{out})^2] \left( \frac{\cos^2 \alpha_{out}}{\cos \alpha_m} \right) \left( \frac{\cos \alpha_{out}}{\cos \alpha_{in}} \right) \quad (21)$$

$$Y_{Tl} = B \frac{l}{h} \left( \frac{\tau}{l} \right)^{0.78} 4(\tan \alpha_{in} - \tan \alpha_{out})^2 \left( \frac{\cos^2 \alpha_{out}}{\cos \alpha_m} \right) \quad (22)$$

166 Where  $\tau$  is the tip clearance,  $h$  is the annulus height, and  $B$  is a constant equals 0.47 for

167 unshrouded blade and 0.37 for shrouded blade.

168

### 169 **4.4. Kacker & Okapuu:**

170 Kacker & Okapuu [20] developed their correlation by adding the influence of shock losses

171 into the loss calculation and new models for profile and secondary losses are presented[24].

$$Y_{total} = \chi_{Re} Y_P + Y_S + Y_{Tl} + Y_{Te} \quad (23)$$

172

173  $\chi_{Re}$  is correction factor and can be calculated using following equation:

$$\chi_{Re} = \left( \frac{R_e}{2 \times 10^5} \right)^{-0.4} \quad \text{for } R_e \leq 2 \times 10^5 \quad (24)$$

$$\chi_{Re} = 1.0 \quad \text{for } 2 \times 10^5 > R_e < 10^6 \quad (25)$$

$$\chi_{Re} = \left( \frac{R_e}{10^6} \right)^{-0.2} \quad \text{for } R_e > 10^6 \quad (26)$$

$$Y_p = 0.914 \left( \frac{2}{3} K_p \chi_i Y_{p(i=0)} + Y_{shock} \right) \quad (27)$$

175           Where  $\chi_i$  is the incidence factor,  $K_p$  is Mach number factor, and  $Y_{shock}$  is losses due  
176 to shocks.

$$K_p = 1 - 1.25(M_{out} - 0.2) \left( \frac{M_{in}}{M_{out}} \right)^2 \quad (28)$$

$$Y_{shock} = 0.75(M_{in,H} - 0.4)^{1.75} \left( \frac{r_H}{r_T} \right) \left( \frac{P_{in}}{P_{out}} \right) \frac{1 - \left( 1 + \frac{\gamma - 1}{2} M_{in}^2 \right)^{\frac{\gamma}{\gamma - 1}}}{1 - \left( 1 + \frac{\gamma - 1}{2} M_{out}^2 \right)^{\frac{\gamma}{\gamma - 1}}} \quad (29)$$

$$M_{in,H} = M_{in} \left( 1 + K * ABS \left( \frac{r_H}{r_T} - 1 \right)^{2.2} \right) \quad (30)$$

177     $K = 1.8$  for stator and  $5.2$  for rotor.

$$Y_s = 0.04 \left( \frac{l}{H} \right) \chi_{AR} [4(\tan \alpha_{in} - \tan \alpha_{out})^2] \left( \frac{\cos^2 \alpha_{out}}{\cos \alpha_m} \right) \left( \frac{\cos \alpha_{out}}{\cos \alpha_{in}} \right) \left[ 1 - \left( \frac{l_x}{H} \right)^2 (1 - K_p) \right] \quad (31)$$

178

179    The trailing edge loss coefficient can be calculated as:

$$Y_{Te} = \frac{\left[ 1 + \frac{\gamma - 1}{2} M_{out}^2 \left( \frac{1}{1 - \Delta E_{Te}} - 1 \right) \right]^{-\gamma/\gamma - 1} - 1}{1 - \left( 1 + \frac{\gamma - 1}{2} M_{out}^2 \right)^{-\gamma/\gamma - 1}} \quad (32)$$

180

181    For unshrouded blade the tip leakage is calculated by:

$$\Delta\eta = 0.93 \left(\frac{r_T}{r_m}\right) \left(\frac{1}{H \cos\alpha_{out}}\right) \eta_o \Delta\tau \quad (33)$$

182

183 Where  $\Delta\eta$  is the variation of efficiency with and without clearance, and  $\eta_o$  is the efficiency  
 184 with zero clearance.

185 For the shrouded blades the leakage losses can be calculated using the following  
 186 equation:

$$Y_k = 0.37 \frac{c}{h} \left(\frac{k'}{c}\right)^{0.78} 4(\tan\alpha_{in} - \tan\alpha_{out})^2 \left(\frac{\cos^2\alpha_{out}}{\cos^3\alpha_m}\right) \quad (34)$$

187

188 Where  $k'$  = the effective tip clearance.

189

## 190 **5. CFD Modelling and Losses Prediction:**

191 Due to the cost of performing experimental tests and as a result of rapid increase in  
 192 computing power, CFD has become an alternative powerful tool for understanding flow  
 193 characteristics in turbo-machines [25, 26]. CFD can provide all the flow features, pressure  
 194 distribution, and aerodynamic characteristics for turbine blades which enable the loss  
 195 coefficients to be determined and compared to those calculated using equations 8-10. In this  
 196 study, full CFD analysis for micro scale axial turbine was carried out using ANSYS CFX 15  
 197 which is based on finite volume technique to solve flow governing equations. Shear Stress  
 198 Transport (SST)  $k-\omega$  turbulent model was chosen for the simulation due its capability of near-  
 199 wall treatment [27].

200 From one dimensional mean line code the turbine stage geometry for both nozzle and  
 201 rotor were defined and constructed through ANSYS Blade-Gen. Using CFX Turbo-Grid the  
 202 domain mesh was generated as shown in Figure 2.

203

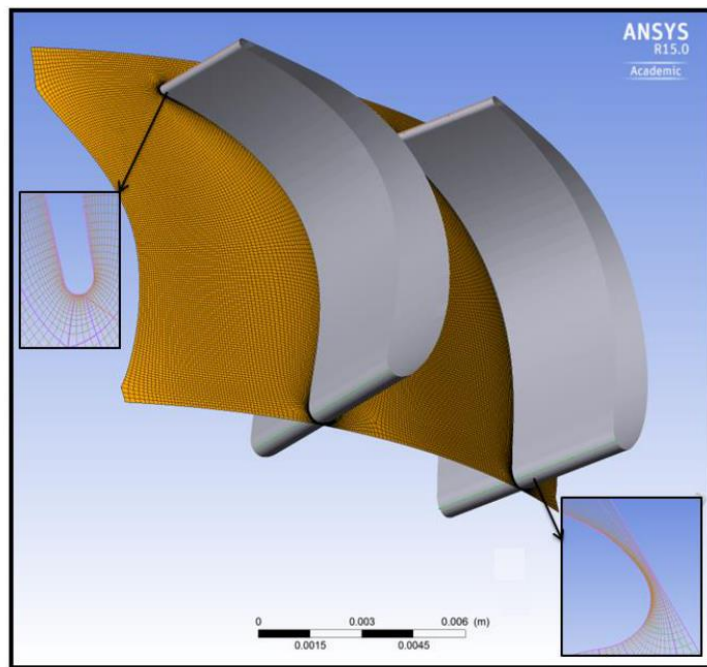


**Figure 2: Mesh Generation (Fine 650,000 cells)**

In order to validate the CFD analysis and as a result of unavailable experimental data for small scale axial turbine, the simulation was carried out for the large scale axial turbine geometry and the experimental data published by Wei [26] using the same geometrical parameters and boundary conditions. Figure 3 shows the predicted (CFD) efficiency compared to the experimental one with +/- 10% deviations.

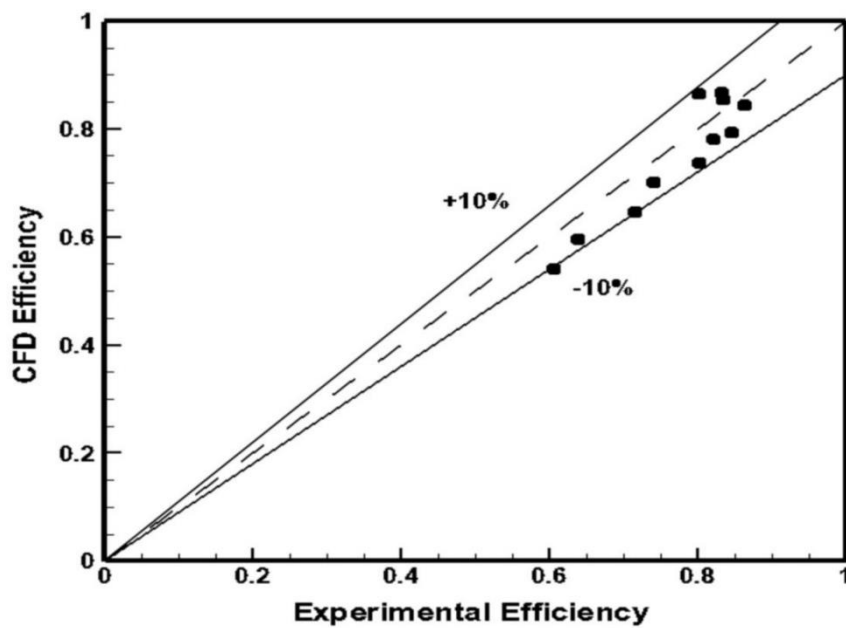


**Figure 3: CFD Model Validation**

229

## 230 6. Turbine Design Optimization for Minimum Loss:

231 Selecting the turbine blade profile which produces minimum losses is a multi-iterative  
232 and complex task which requires the application of advanced optimization techniques or  
233 expensive actual test of many blade profiles. The integration of the optimization algorithm  
234 with simulation software can be used as an effective tool for turbine design optimization. The  
235 advantage of this approach is that the design candidates can be generated using design of  
236 experiments method with a high flexibility in choosing design parameters levels and different  
237 optimization criteria can be applied [26, 28, 29].

238 To obtain optimum blade geometry, the optimization process requires a full definition  
239 of all blade geometrical parameters and constrains. Well known method of aerofoil cross  
240 section parameters definition is published by Pritchard [30] who described the blade profile  
241 by eleven parameters including flow angles, axial blade chord, turning angle, leading edge  
242 radius and trailing edge thickness as shown in Figure 4.

243

244

245

246

247

248

249

250

251

252

253

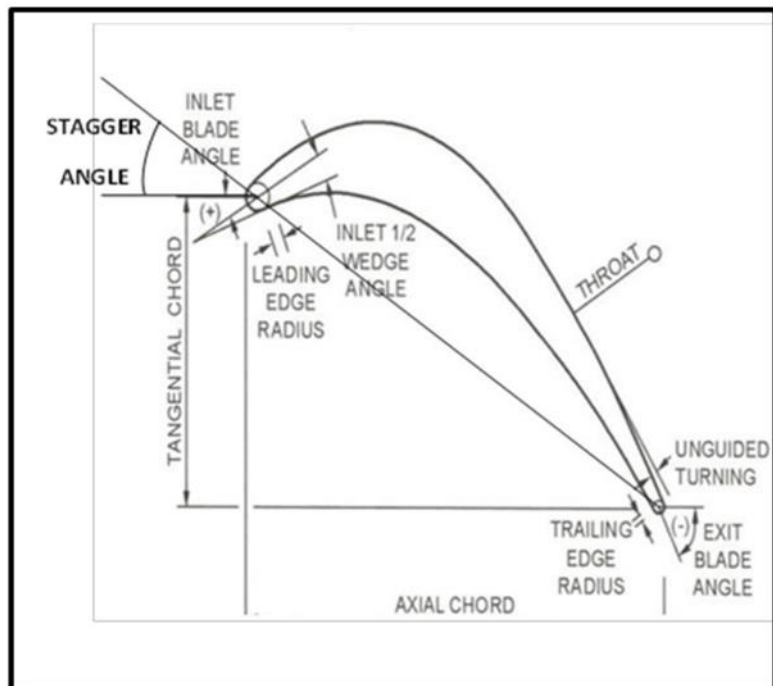


**Figure 4: Blade Geometry Parameters [6]**

254

255 A three-dimensional steady flow simulation using ANSYS CFX15 was created for  
256 blade profile optimization. ANSYS CFX design explorer can use design of experiments  
257 (DoE) which is used to generate sufficient data (design points) based on the number of input  
258 and output parameters including the interactions between design variables. The DoE  
259 approach can be applied for numerical modelling systems to predict the output response as a  
260 function of design parameters which can be optimized for maximum or minimum output  
261 response. The design explorer also applies response surface method (RSM) which is used in  
262 design optimization to build a relationship between independent design variables (input  
263 parameters) and the output response (output parameter) [31]. The general optimizations  
264 strategy using ANSYS CFX is described by a flowchart shown in Figure 5.

265

266

267

268

269

270

271

272

273

274

275

276

277

278

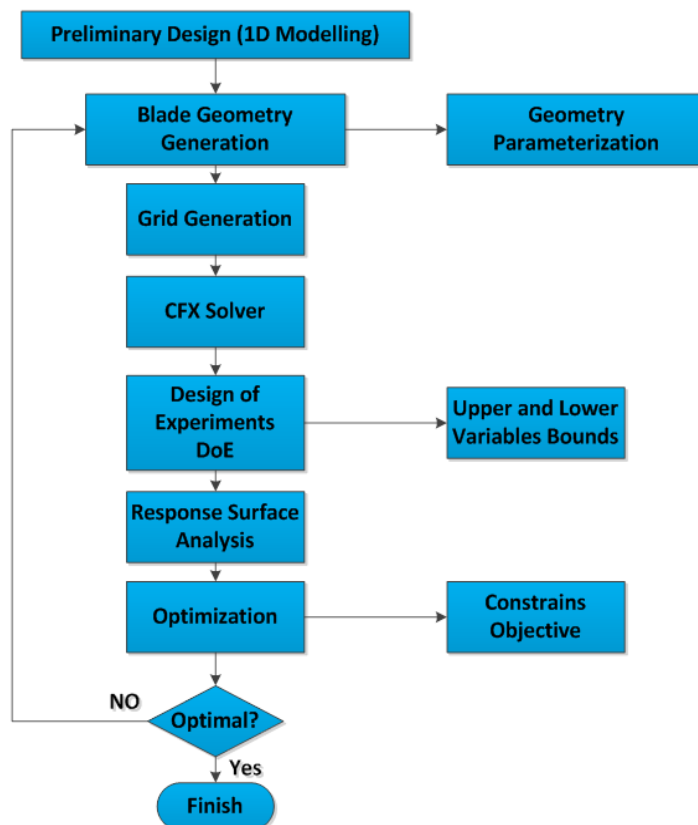


**Figure 5: Optimization Strategy Description**

## 279 7. Multi-objective Genetic Algorithm (MOGA):

280 In axial turbine development, the designer needs to optimize the blade profile for  
281 maximum efficiency. The turbine blade profile and flow path design can be optimized at the  
282 mean radius using genetic algorithms (GAs) to identify blade aerodynamic geometry for  
283 maximum performance [32]. However, the turbine design optimization for higher efficiency  
284 is multi-objective problem. Multi- objective genetic algorithm is an evolutionary algorithm  
285 with several objective functions which are optimised simultaneously and subjected to  
286 inequality and equality constrains [33]. According to Coello et al. mathematically MOGA  
287 can be formulated in a vector form as [34-36]:

288 The objective function vector:  $F(X) = [f_1(X), f_2(X), \dots \dots f_k(X)]^n$

289 Subject to:  $g_i(X) \leq 0 \quad i = \{1, \dots, m\}$

290  $h_j(X) = 0 \quad j = \{1, \dots, p\}$

291 Where k is the dimensional space of the objective functions  $g_i(X)$  is the inequality  
292 constrains, and  $h_j(X)$  is the equality constrains.

293 In this study, there are two objective functions considered in Multi-objective optimisation  
294 algorithm. The first objective function (to be maximized) is turbine total to total efficiency  
295 ( $\eta_{tt}$ ), and the second objective function (to be minimised) is total pressure loss through  
296 turbine rotor ( $Y_R$ ).

$$\text{Maximize:} \quad OF_1 = \eta_{tt} = \frac{h_{01} - h_{03}}{h_{01} - h_{03SS}} \quad (35)$$

$$\text{Minimize:} \quad OF_2 = Y_R = \frac{(P_{02 \text{ rel}} - P_{03 \text{ rel}})}{(P_{01 \text{ rel}} - P_3)} \quad (36)$$

297 **8. Results and Discussion:**

298

299 **8.1. CFD Loss Prediction:**

300 This section presents a comparison between losses prediction using published correlations  
301 and losses obtained based on CFD simulation using ANSYS CFX for the operating  
302 conditions which are provided in Table1 and the total pressure loss was extracted from CFD  
303 and calculated using equation (7).

304

305 **Table (1):** Turbine Design Parameters:

Power output ( <i>kW</i> )	5	Total inlet temperature ( <i>K</i> )	360
Mass flow rate ( <i>kg/sec</i> )	0.3225	Inlet relative flow angle ( <i>degree</i> )	59.04
Shaft speed ( <i>rpm</i> )	14000	Exit absolute flow angle ( <i>degree</i> )	65.12
Total inlet Pressure ( <i>kpa</i> )	200	Hub-tip ratio	0.75
Rotor Mean radius ( <i>mm</i> )	35	Rotor span ( <i>mm</i> )	10
Solidity	1.613	LE Wedge Angle( <i>degree</i> )	22.5
Rotor Stagger Angle ( <i>degree</i> )	19.5	Camber Angle ( <i>degree</i> )	52.14

306

307

308 Figures 6 and 7 present the predicted rotor total loss coefficient for different rotational  
309 speeds (5,000-25,000) and a range of pressure ratios (1.5-3.5) which represents both on and  
310 off design conditions. The loss was predicted using Came & Dunham, Kacker & Okapuu, and  
311 Ainely colorations and compared with loss obtained by CFD simulation.



312

313

314

315

316

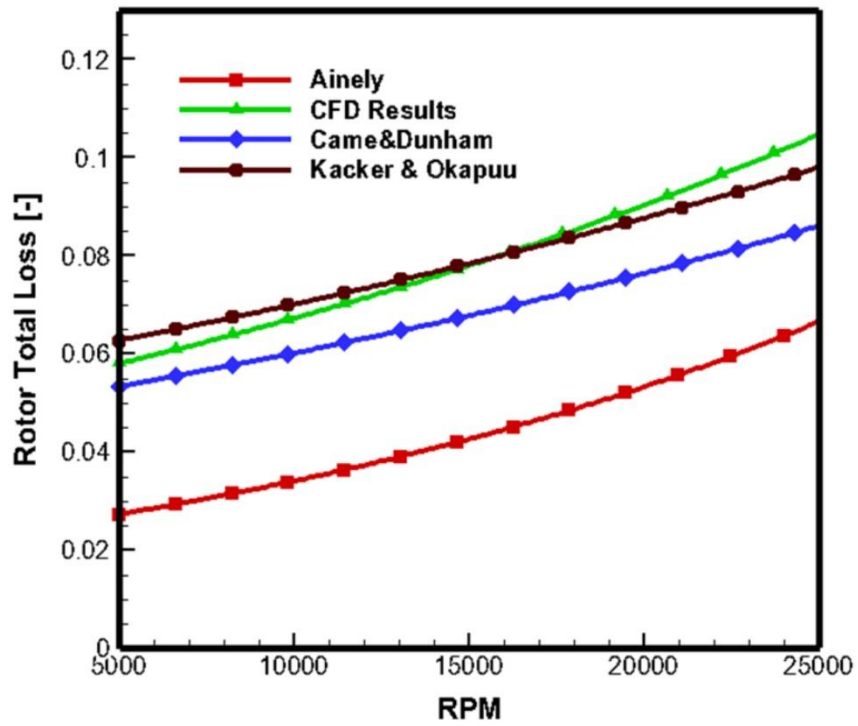
317

318

319

320

321



322

323

Figure 6: Rotor Total Loss Coefficient for different RPM

324

325

326

327

328

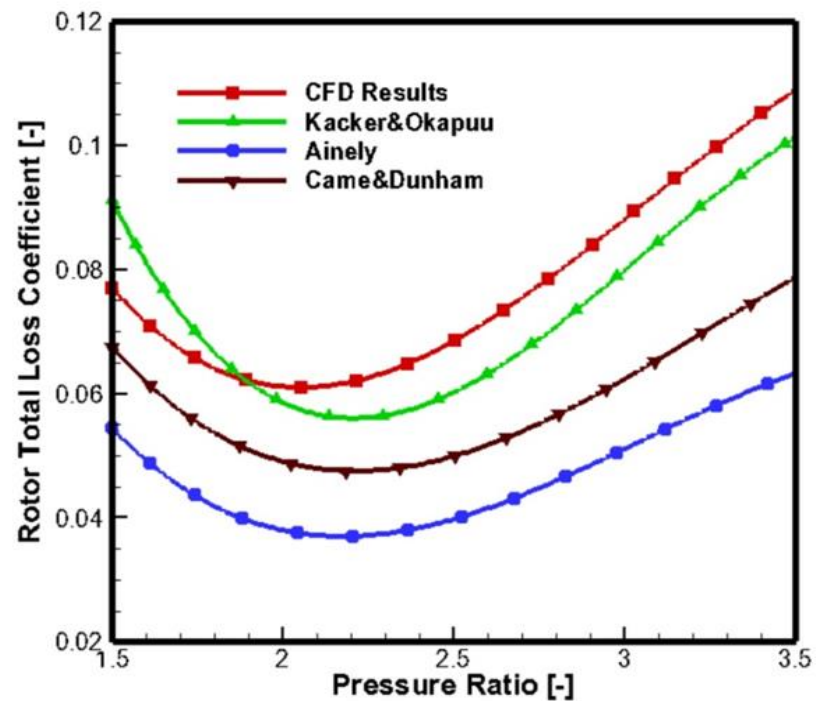
329

330

331

332

333

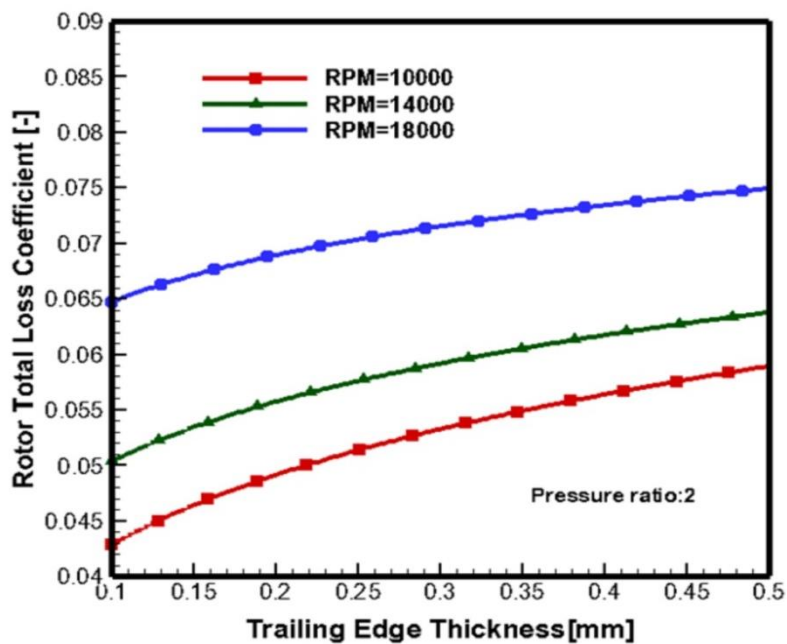


334

335

Figure 7: Rotor Total Loss Coefficient for different Pressure Ratio

336 It is clear from these figures that Kacker & Okapuu predicted losses are the closest to CFD  
 337 results, while results by Ainely & Mathieson approach are the lowest loss values.  
 338 Furthermore, Kacker & Okapuu Model was close to CFD near to design point ( $pr=2$ ,  
 339  $RPM=14,000$ ) and these results deviates for off design conditions. Therefore, the CFD was  
 340 used to carry out a parametric analysis to study the effects of turbine blade geometry like  
 341 trailing edge thickness as shown in Figure 8.



352 **Figure 8: Rotor Total Loss Coefficient vs. Trailing Edge Thickness**

354 The impact of blade incidence angle ( $i$ ) (the difference between inlet flow angle and blade  
 355 angle) on loss generation is presented in Figure 9. It can be seen that the rotor total losses  
 356 increases gradually for both positive incidence (0 to  $+15^\circ$ ) and negative incidence (0 to  $-15^\circ$ ).  
 357 As a result of the significant impact of blade incidence on loss generation, it is important to  
 358 identify the influence of leading edge geometry on loss generation.

359  
360  
361  
362  
363  
364  
365  
366  
367  
368  
369  
370  
371  
372  
373  
374  
375  
376  
377  
378  
379

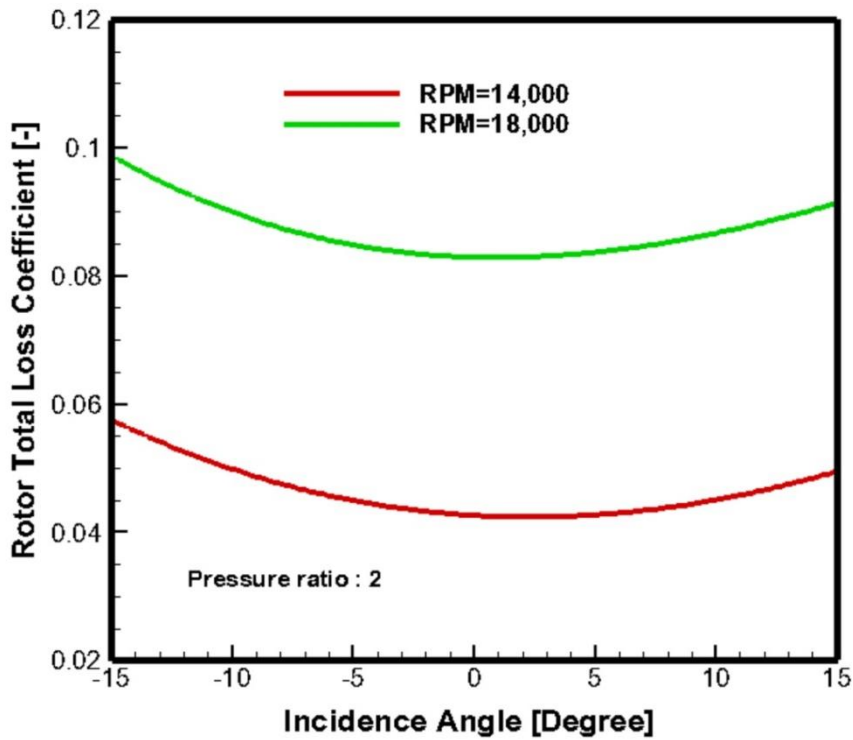
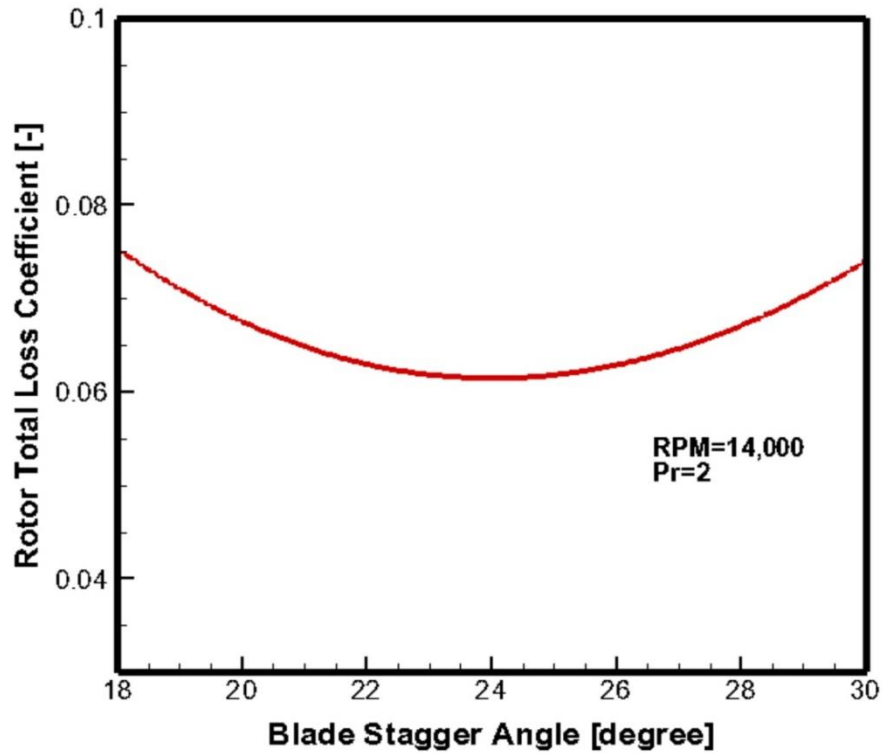


**Figure 9: Rotor Total Loss Coefficient vs. Incidence Angle**

### 8.2. Optimization Results:

From the results of loss prediction, it is obvious that the loss development is correlated with the blade profile geometry parameters. For efficient aerodynamic blade profile with minimum loss, the design optimization was performed through 3D CFD simulation and MOGA. The turbine blade geometric parameters were varied for different operating conditions to identify the optimum blade thickness distribution that satisfy the design goals with minimum total loss and higher performance.

380 Figure (10) shows the change in rotor total loss due to the variations in blade stagger angle. It  
381 shows that for a 5 kW compressed air axial turbine the best stagger angle is 21.48°. The  
382 stagger angle is one of critical parameters due to its significantly impact on the thickness  
383 distribution, throat area, and turbine overall performance.



395 **Figure 10: Rotor Total Loss Coefficient for different Stagger Angle**

396 CFD modelling of the original blade baseline design and optimized blades (Figure 11) was  
397 carried out and results are provided in terms of entropy generation. The loss distribution on  
398 turbine blades can be evaluated by entropy generation as the key feature that measures  
399 aerodynamic loss through turbine passage.

400  
401  
402

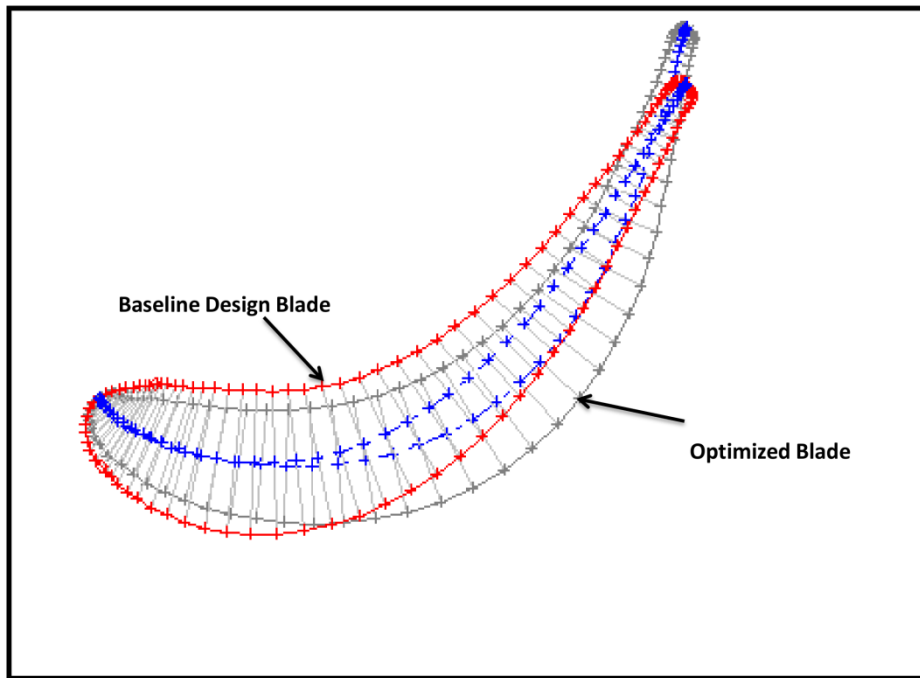


**Figure 11: Original and Optimized Blade Profiles**

Figure (12) shows the entropy generation contours of both baseline turbine design and optimized turbine. By comparing these two entropy contours, it can be observed clearly that the optimization approach could reduce maximum entropy generation rate from (216 J/kg.K) to (136 J/kg.K). This comparison between the baseline blade design and the optimised blade shows the dominant effect of blade thickness distribution on turbine aerodynamic performance and loss development. As can be seen, the optimization approach could reduce the flow loss through blade geometry variations (blade profile redesign) as a result of the dependence of boundary layer development, pressure, and flow velocity on blade surface curvature. The blade thickness distribution is characterized by blade stagger angle, leading and trailing edge geometries. Through the optimization, the flow separation at LE and TE can be avoided. Also the pressure distribution can be improved along the blade surface to overcome local flow acceleration and deceleration.

428  
429  
430  
431  
432  
433  
434  
435  
436  
437  
438  
439  
440  
441  
442  
443  
444  
445  
446  
447  
448  
449  
450  
451  
452

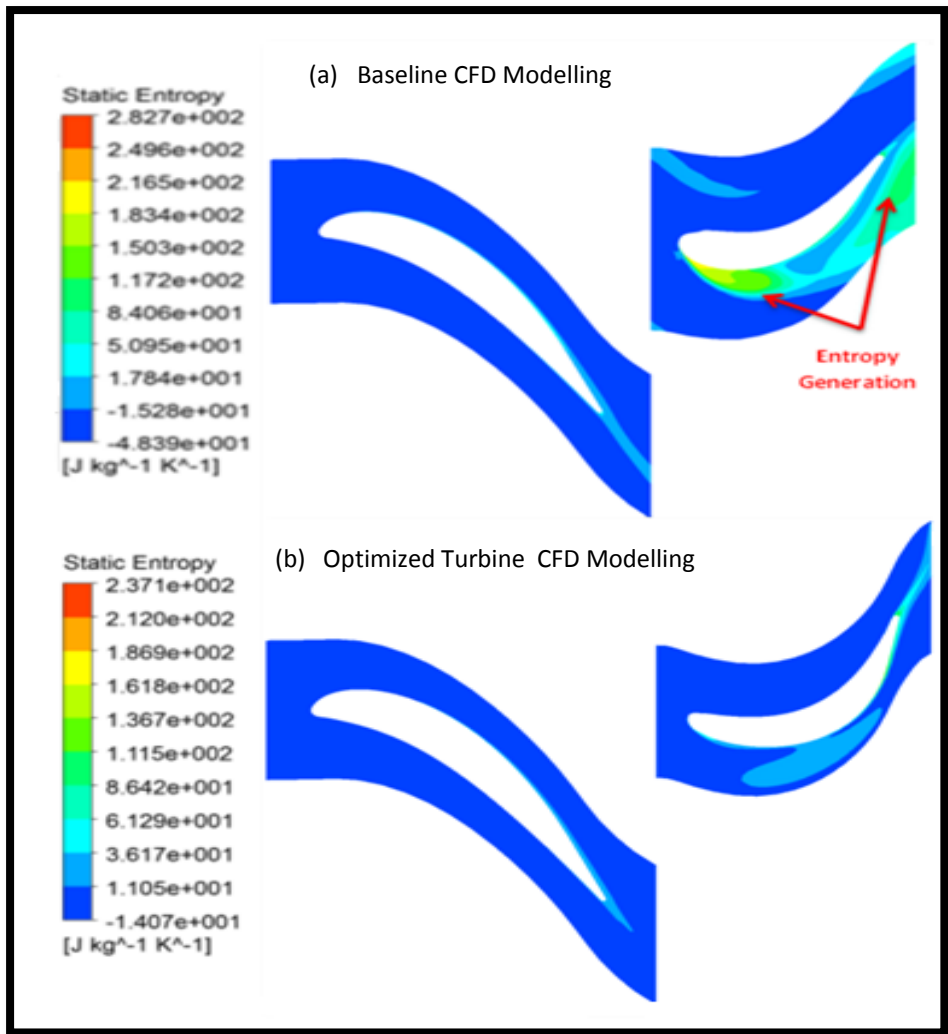


**Figure 12: Entropy Generation contours: (a) Baseline Design (b) Optimized Design**

Table (2) provides a detailed description of blade geometrical parameters and the performance of the turbine design produced through iterative parametric CFD analysis and optimised turbine for the 5kW compressed air axial turbine indicating a 12.34% increase in efficiency.

453 **Table (2):** CFD-MOGA Optimization Results:

Minimize P4;Pressure Loss	Goal, Minimize Mize P4 (Default importance); Strict Constraint	
Seek P5 = 5000 W	Goal, Seek P5 = (Default Importance)	
Optimization Method	The MOGA method (Multi-Objective Genetic Algorithm)	
Configuration	100 samples per iteration	
	<b>Baseline Design</b>	<b>Optimized Design</b>
Stager angle (m)	19.50	23.48
Number blades	22	18
Tip Clearance (m)	0.001268775	0.00098821
Leading. Major radius (m)	0.000227	0.000386
Leading. Minor radius (m)	0.0001274	0.0001133
Trailing. Major radius (m)	0.0005	0.00033
Trailing. Minor radius (m)	0.0003	0.00013
Wedge Angle (degree)	21.5	18.07
Stator-Rotor Gap (mm)	5.0	4.15
Throat (m)	0.004077	0.0032628
Rotor Pressure Loss Coeff.	0.087512	0.060234
Effs out (Total-to-Total)	76.8479	87.7861
Output Power (W)	4977.407	4463.227

454  
455  
456

**9. Conclusion:**

457 For efficient small scale air driven axial turbines, the loss predictions are crucial for  
458 design and development. The published conventional loss prediction models are developed  
459 for large scale turbines. Therefore there is a need for an effective approach to predict and  
460 minimise such losses for the small scale axial turbines. This work compares the predicted  
461 losses based on published literature correlations with those from CFD simulations. Results

462 showed that the Kacker & Okapuu model predicted the closest values to the CFD simulation  
463 results and hence can be used to predict losses for small axial turbines. Also, the combined  
464 3D CFD with MOGA optimization technique can be used to minimise total loss coefficient  
465 and produce the optimum design parameters in terms of blade stagger angle, stator to rotor  
466 spacing and number of blades, etc. This combined approach can be used to achieve higher  
467 total to total efficiency with up to 12.48% increase highlighting the potential of this  
468 developed technique.

469

#### 470 **References:**

- 471 1. Le Roux, W.G., T. Bello-Ochende, and J.P. Meyer, *The efficiency of an open-cavity tubular*  
472 *solar receiver for a small-scale solar thermal Brayton cycle*. Energy Conversion and  
473 Management, 2014. **84**: p. 457-470.
- 474 2. Qiu, G., H. Liu, and S. Riffat, *Expanders for micro-CHP systems with organic Rankine cycle*.  
475 Applied Thermal Engineering, 2011. **31**(16): p. 3301-3307.
- 476 3. Quoilin, S. and V. Lemort. *Technological and economical survey of organic Rankine cycle*  
477 *systems*. in *European conference on Economics and management of energy in industry*. 2009.
- 478 4. Hasan, N.S., et al., *Review of storage schemes for wind energy systems*. Renewable and  
479 Sustainable Energy Reviews, 2013. **21**: p. 237-247.
- 480 5. Saravanamuttoo, H.I.H., G.F.C. Rogers, and H. Cohen, *Gas turbine theory*. 2001: Pearson  
481 Education.
- 482 6. Moustapha, H., et al., *Axial and radial turbines*. Vol. 2. 2003: Concepts NREC Wilder, VT.
- 483 7. Dixon, S.L. and C. Hall, *Fluid mechanics and thermodynamics of turbomachinery*. 2013:  
484 Butterworth-Heinemann.
- 485 8. Yahya, S., *Turbines compressors and fans*. 2010: Tata McGraw-Hill Education.
- 486 9. Sieverding, C., *Recent progress in the understanding of basic aspects of secondary flows in*  
487 *turbine blade passages*. Journal of Engineering for Gas Turbines and Power, 1985. **107**(2): p.  
488 248-257.
- 489 10. Ainley, D. and G. Mathieson, *An Examination of the Flow and Pressure Losses in Blade Rows*  
490 *of Axial-Flow Turbines*. 1951: HM Stationery Office.
- 491 11. Dunham, J. and P. Came, *Improvements to the Ainley-Mathieson method of turbine*  
492 *performance prediction*. Journal of Engineering for Gas Turbines and Power, 1970. **92**(3): p.  
493 252-256.
- 494 12. Craig, H. and H. Cox, *Performance estimation of axial flow turbines*. Proceedings of the  
495 Institution of Mechanical Engineers, 1970. **185**(1): p. 407-424.
- 496 13. Ainley, D. and G. Mathieson, *A method of performance estimation for axial-flow turbines*.  
497 1951: Citeseer.
- 498 14. Moustapha, S., S. Kacker, and B. Tremblay, *An improved incidence losses prediction method*  
499 *for turbine airfoils*. Journal of Turbomachinery, 1990. **112**(2): p. 267-276.
- 500 15. Benner, M., S. Sjolander, and S. Moustapha, *Influence of leading-edge geometry on profile*  
501 *losses in turbines at off-design incidence: experimental results and an improved correlation*.  
502 Journal of turbomachinery, 1997. **119**(2): p. 193-200.
- 503 16. Bullock, R., *Analysis of Reynolds number and scale effects on performance of*  
504 *turbomachinery*. Journal of Engineering for Gas Turbines and Power, 1964. **86**(3): p. 247-256.



- 505 17. Klonowicz, P., et al., *Significance of loss correlations in performance prediction of small scale,*  
506 *highly loaded turbine stages working in Organic Rankine Cycles.* Energy, 2014. **72**: p. 322-  
507 330.
- 508 18. Macchi, E. and G. Lozza. *Comparison of Partial vs Full Admission for Small Turbines at Low*  
509 *Specific Speeds.* in *ASME 1985 International Gas Turbine Conference and Exhibit.* 1985.  
510 American Society of Mechanical Engineers.
- 511 19. Macchi, E. and A. Perdichizzi, *Efficiency prediction for axial-flow turbines operating with*  
512 *nonconventional fluids.* Journal of Engineering for Gas Turbines and Power, 1981. **103**(4): p.  
513 718-724.
- 514 20. Angelino, G., L. De Luca, and W.A. Sirignano, *Modern Research Topics in Aerospace*  
515 *Propulsion: In Honor of Corrado Casci.* 2012: Springer Science & Business Media.
- 516 21. Wei, N., *Significance of loss models in aerothermodynamic simulation for axial turbines.* 2000.
- 517 22. Fielding, L., *Turbine design: the effect on axial flow turbine performance of parameter*  
518 *variation.* 2000.
- 519 23. Xiao, X., A.A. McCarter, and B. Lakshminarayana, *Tip clearance effects in a turbine rotor: part*  
520 *I—pressure field and loss.* Journal of turbomachinery, 2001. **123**(2): p. 296-304.
- 521 24. Kacker, S. and U. Okapuu, *A mean line prediction method for axial flow turbine efficiency.*  
522 *Journal of Engineering for Gas Turbines and Power,* 1982. **104**(1): p. 111-119.
- 523 25. Aldi, N., et al., *Numerical Analysis of the Effects of Surface Roughness Localization on the*  
524 *Performance of an Axial Compressor Stage.* Energy Procedia, 2014. **45**: p. 1057-1066.
- 525 26. Janjua, A.B., M.S. Khalil, and M. SAEED, *Blade profile optimization of kaplan turbine using cfd*  
526 *analysis.* 2013.
- 527 27. Rahbar, K., S. Mahmoud, and R.K. Al-Dadah, *Mean-line modeling and CFD analysis of a*  
528 *miniature radial turbine for distributed power generation systems.* International Journal of  
529 Low-Carbon Technologies, 2014: p. ctu028.
- 530 28. Tveit, T.-M. and C.-J. Fogelholm, *Multi-period steam turbine network optimisation. Part I:*  
531 *Simulation based regression models and an evolutionary algorithm for finding D-optimal*  
532 *designs.* Applied Thermal Engineering, 2006. **26**(10): p. 993-1000.
- 533 29. Sasaki, D., S. Obayashi, and H.-J. Kim. *Evolutionary algorithm vs. adjoint method applied to*  
534 *sst shape optimization.* in *The Annual Conference of CFD Society of Canada, Waterloo.* 2001.
- 535 30. Pritchard, L. *An eleven parameter axial turbine airfoil geometry model.* in *ASME 1985*  
536 *International Gas Turbine Conference and Exhibit.* 1985. American Society of Mechanical  
537 Engineers.
- 538 31. Myers, R.H., A.I. Khuri, and W.H. Carter, *Response surface methodology: 1966–1988.*  
539 *Technometrics,* 1989. **31**(2): p. 137-157.
- 540 32. Qin, X., et al., *Optimization for a steam turbine stage efficiency using a genetic algorithm.*  
541 *Applied Thermal Engineering,* 2003. **23**(18): p. 2307-2316.
- 542 33. Jamali, A., P. Ahmadi, and M.N. Mohd Jaafar, *Optimization of a novel carbon dioxide*  
543 *cogeneration system using artificial neural network and multi-objective genetic algorithm.*  
544 *Applied Thermal Engineering,* 2014. **64**(1–2): p. 293-306.
- 545 34. Coello, C.A.C., D.A. Van Veldhuizen, and G.B. Lamont, *Evolutionary algorithms for solving*  
546 *multi-objective problems.* Vol. 242. 2002: Springer.
- 547 35. Yang, W. and R. Xiao, *Multiobjective optimization design of a pump–turbine impeller based*  
548 *on an inverse design using a combination optimization strategy.* Journal of Fluids  
549 Engineering, 2014. **136**(1): p. 014501.
- 550 36. Olszewski, P., *Genetic optimization of steam multi-turbines system.* Applied Thermal  
551 Engineering, 2014. **71**(1): p. 230-238.  
552